

RSC Advances



This is an *Accepted Manuscript*, which has been through the Royal Society of Chemistry peer review process and has been accepted for publication.

Accepted Manuscripts are published online shortly after acceptance, before technical editing, formatting and proof reading. Using this free service, authors can make their results available to the community, in citable form, before we publish the edited article. This *Accepted Manuscript* will be replaced by the edited, formatted and paginated article as soon as this is available.

You can find more information about *Accepted Manuscripts* in the [Information for Authors](#).

Please note that technical editing may introduce minor changes to the text and/or graphics, which may alter content. The journal's standard [Terms & Conditions](#) and the [Ethical guidelines](#) still apply. In no event shall the Royal Society of Chemistry be held responsible for any errors or omissions in this *Accepted Manuscript* or any consequences arising from the use of any information it contains.



Journal Name

ARTICLE

High selectivity and sensitivity fluorescent sensing melamine based on the combination of fluorescent chemosensor with molecularly imprinted polymers

Received 00th January 20xx,

Kejin Sun,^a Qiliang Deng,^{a*} Ting Guo, Rina Su, Yuchen Gu and Shuo Wang*

Accepted 00th January 20xx

DOI: 10.1039/x0xx00000x

www.rsc.org/

In this study, a sensitive and efficient approach was developed for the determination of melamine (MEL) based on the combination of molecularly imprinted polymers (MIPs) with synthesized fluorescent chemosensor. Fluorescent chemosensor was designed ingeniously based on the open loop of Rhodamine B (RB) derivative. The MIPs were prepared by precipitation polymerization with MEL as template, nano-CaCO₃ as porogenic agent, ethyleneglycoldimethacrylate as crosslinking agent and methacrylic acid as functional monomer. Specific recognition ability of MIPs was investigated by static adsorption, kinetic adsorption, selective, and competitive adsorption, respectively. The resulted materials showed outstanding affinity and selectivity to MEL. The imprinting factor of 3.072 could be obtained. The fluorescence intensity of chemosensor displayed an outstanding linear relationship to the concentration of MEL in the range of 6.25×10^{-4} – 8×10^{-2} mmol/L. The limit of detection (LOD) was found to be 1.55×10^{-4} mmol/L. The recovery for MEL was in the range of 86.48–89.12% for the milk samples, with RSDs ranging from 3.18 to 4.91%. The proposed approach was successfully applied to determine MEL in milk samples.

Introduction

Melamine (MEL, C₃H₆N₆) is an industrially important chemical, and has been widely and massively used in the production of resins, glues and plastics as heat tolerant.¹ Because MEL has a substantial proportion of nitrogen content (ca. 66% w/w) and low cost, it is usually added into milk and other products aiming to cause a false increase in apparent protein content in worldwide.² Experimental studies show that MEL can interact with cyanuric acid, and lead to an insoluble matter, which damage to urinary and reproductive system in children and babies especially.³ In the year of 2008, melamine-tainted milk powder caused the death of some infants in china.⁴ According to world health organization (WHO), the maximum residue level for MEL is 1 mg/kg in infant formula.⁵ However, it is difficult to detect low levels of MEL in the complex milk matrix. Therefore, a credible and sensitive approach for detecting MEL residues in infant formula and milk powder is urgent.

So far, lots of analytical approaches have been developed for the determination of MEL, such as gas chromatography (GC),⁶ high performance liquid chromatography (HPLC),⁷ electrospray

ionization tandem mass spectrometry (ESI-MS),⁸ surface enhanced Raman spectroscopy (SERS)⁹ and capillary zone electrophoresis (CZE).¹⁰ These approaches have some advantages, but also meet some disadvantages such as high-cost analytical equipments, complicated sample pre-concentration treatments and extensive use of harmful organic solvents. Recently, fluorescent approaches including fluorescence enhancement and fluorescence quenching^{11–13} have been reported. Among them, the fluorescence turn-on mode is fascinating due to excellent sensitivity, such as fluorescence nanomaterials.¹⁴ In addition to fluorescent nanomaterials, fluorescent dye of RB derivative was also found to have a new type of turn-on mode for melamine in the experiment.

Molecular imprinting technology is an interesting approach to synthesize materials with molecular recognition sites, which are complementary in shape, dimension and functionality with the target molecule, and the resulted materials exhibit extraordinary high affinity and selectivity to the given target.¹⁵ MIPs have received much attention, particularly with respect to the separation and solid phase extraction,¹⁶ and for their applications in drug delivery and release.¹⁷

Different methods have been employed to prepare MIPs based on MEL, such as precipitation polymerization,^{3,18} bulk polymerization¹⁹ and surface photopolymerization.²⁰ MIPs prepared by bulk polymerization need to be crushed, ground and sieved, which is time-consuming and easy to waste. Due to three-dimensional transformation into two-dimensional, the loss of the dimension makes the adsorption capacity of MIPs prepared by surface photopolymerization decrease.

Key Laboratory of Food Nutrition and Safety, Ministry of Education, Tianjin Key Laboratory of Food Nutrition and Safety, College of Chemical Engineering and Materials Science, Tianjin University of Science and Technology, Tianjin 300457, China. E-mail: s.wang@tust.edu.cn; yhdq@tust.edu.cn; Fax: (+86 22) 60912489; Tel: (+86 22) 60912493

^a These authors contributed equally to this work

*Corresponding author: Shuo Wang or Qiliang Deng

†Electronic Supplementary Information (ESI) available: Fig.S1: ¹H NMR, ¹³C NMR and LC-MS spectroscopy of RBH. Fig.S2: ¹H NMR, ¹³C NMR and LC-MS spectroscopy of RB1. See DOI: 10.1039/x0xx00000x

Precipitation polymerization has received increasing attention, because this kind of MIPs exhibits high selectivity, and the shape of the polymer microspheres is uniform and the size is easy to control.

Herein, we assume to recognize and combine MEL by using MIPs as adsorbing material, MEL will be separated from complexly coexisting substances and selectively adsorbed on the MIPs materials, followed by detection with a new fluorescence probe of rhodamine B derivative, called RB1 for short. RB1 exhibits very low fluorescence background, which provides favorable conditions for the fluorescence enhancement. The combination of both enable that the present approach is further applied to detect MEL in real samples to demonstrate its practicality. However, to the best of our knowledge, this is the first time that fluorescent chemosensor for detection of MEL after enriched and separated by MIPs is reported.

Experiment section

Materials and measurements

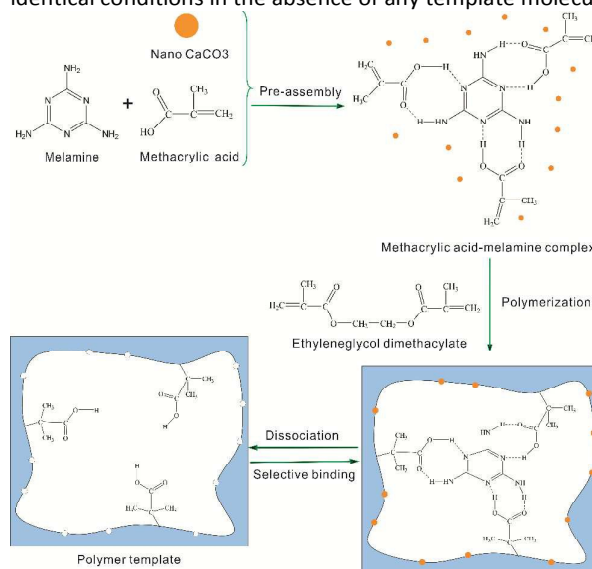
Rhodamine B (RB) was purchased from Sigma-Aldrich (Shanghai, China). Melamine (MEL), benzoguanamine (BEN) and cyromazine (CYR) were obtained from J&K Chemical (Beijing, China). Ethyleneglycoldimethacrylate (EGDMA) and methacrylic acid (MAA) were purchased from Alfa Aesar (Tianjin, china). Hydrazine hydrate, nano-CaCO₃, citric acid, 2, 2'-Azo-bis-isobutyronitrile (AIBN), methanol, acetonitrile and ethanol were provided by Damao Chemical (Tianjin, China). Chromatographic grade acetonitrile, sodium octane sulfonate and methanol were obtained from Fisher Scientific. The pure milk was purchased from a local supermarket.

Fluorescence spectra were acquired on a Lumina spectrofluorometer (Thermo, USA). Absorption spectra were monitored by an UV-vis spectrophotometer (Thermo, USA). SEM images were performed on a scanning electron microscope (SEM; SU1510; Hitachi, Japan). Thermogravimetric (TG) analysis about thermal stability was performed by a Q50 thermal analyzer (TA, USA). ¹H and ¹³C NMR spectra were measured on a NMR spectrometer with CDCl₃ at 400 MHz (Bruker BioSpin, Switzerland). The HPLC analysis was conducted on Agilent 1260 infinity series equipped with a UV-vis detector, an incubator chamber and a quaternary pump.

Preparation of MIPs

The schematic diagram of the preparation process is shown in Scheme 1. The MIPs were prepared by precipitation polymerization. Briefly, MEL (3.5 mmol, 0.3mL) as template, MAA (3.5 mmol, 0.3mL) as functional monomer, nano-CaCO₃ as porogen, were all added into the mixture of acetonitrile (10 mL) and methanol (50 mL) in a 100 mL of round flask. The round flask was stored at 4 °C refrigerator for 2h to promote the formation of hydrogen bond between the template and the monomer in mixed system. Then, EGDMA (26.5 mmol, 5 mL) as crosslinking agent and AIBN (0.18 mmol, 30 mg) as the initiator were added into the round flask. After purged with nitrogen gas for 15 min, the above pre-polymerization system

was placed in the water-bath at 60 °C for 24h. The obtained polymer particles were subsequently eluted with methanol containing 10% (v/v) acetic acid to remove the template molecules, nano-CaCO₃ and unreacted reagents by soxhlet extraction until no template was detected from the recovered solutions with a UV spectrum ($\lambda = 230$ nm). And then the MIPs were washed with methanol for three times to remove residual acetic acid. Finally, the particles were dried in vacuum oven to constant weight at 40 °C. For comparison, the non-imprinted polymers (NIPs) were also prepared under the identical conditions in the absence of any template molecule.



Scheme 1 Schematic representation of MIPs preparation.

Static adsorption experiments

The static adsorption measurements were carried out by adding certain amounts of MIPs or NIPs in centrifuge tubes containing various concentrations of MEL. Briefly, MIPs or NIPs (20 mg) were mixed with 4 mL of various concentrations of melamine methanol solution (0.1, 0.15, 0.2, 0.3, 0.4, 0.6, 0.8, 0.9, 1.0, 1.2 mmol/L) in 5 mL centrifuge tubes, and then oscillated for 24 h at room temperature. After centrifugation for 10 min at 2000 rpm, the concentration of free MEL in the supernatant was analyzed with UV detection at the wavelength of 230 nm.

Adsorption kinetics experiments

MIPs or NIPs particles (20mg) were added into the centrifugal tubes containing 4 mL of 0.9 mmol/L of MEL. The centrifugal tubes were oscillated gently and the supernatant was then taken out at different intervals of 5, 10, 20, 30, 40, 60, 80, 120, 180, 210 and 240 min at room temperature to measure the concentration of MEL with UV absorption spectroscopy.

Selective and competitive adsorption experiments

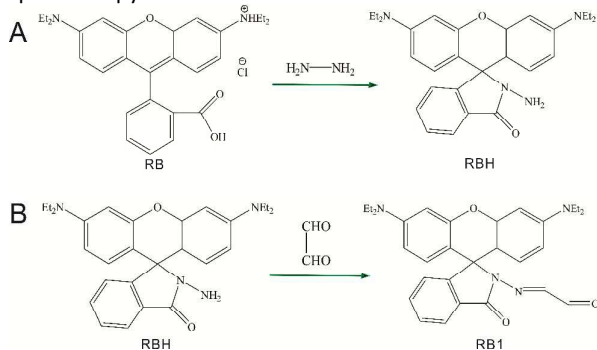
Selective adsorption recognition was measured to make use of several substances with similar chemical structure to MEL, such as benzoguanamine (BEN) and cyromazine (CYR). The experiment was finished by adding MIPs or NIPs particles (20mg) into the centrifugal tubes containing 4 mL of 0.3

mmol/L of MEL (or BEN or CYR) methanol solution, respectively. The centrifugal tubes were oscillated gently for 24 h at room temperature. The suspension was separated through centrifugation and then MEL in suspension solution was detected by UV absorption spectroscopy.

Competitive adsorption recognition ability was evaluated by adding MIPs or NIPs (20mg) into the centrifugal tubes containing 4 mL of the mixture of MEL, BEN and CYR with the concentration of each 0.3 mmol/L. The centrifugal tubes were oscillated gently for 24 h at room temperature. The suspension was separated through centrifugation and then tested with HPLC. HPLC conditions: chromatographic column: C18 (5 μ m particle size, 150 \AA , 250 mm \times 4.6 mm); mobile phase: buffer solution (sodium octane sulfonate/citric acid, pH 3.00)/acetonitrile = 85/15 (v/v); flow rate: 1.0 mL/min; detection wavelength: 240nm; injection volume: 20 μ L.

Synthesis of RB1

RB1 was synthesized referencing to the literature²¹ and the synthetic route was shown in Scheme 2. 0.5 g of RB was dissolved in 20 mL of ethanol through ultrasound in a single flask (150 mL), and then 1 mL of hydrazine hydrate (80%, v/v) was added while agitating vigorously. In the heating reflux system, the mixed solution was heated at 85 $^{\circ}\text{C}$ until the pink color translated to transparent (about 24 h; Scheme 2A). The mixture was cooled down, and then the remaining ethanol was evaporated by a rotary evaporator at reduced pressure. Afterwards, 20 mL of ultrapure water and 20 mL of dichloromethane were all added to the mixture. The under layer consisting of dichloromethane and rhodamine B hydrazide (RBH) was then separated and evaporated under vacuum to eliminate the dichloromethane, and RBH was obtained. Then 0.3 g of RBH, 10 mL of absolute ethanol and 1.5 mL of 40% glyoxal were all appended into a single flask (100 mL), and the mixed solution was stirred for 8 h under nitrogen protection at room temperature (Scheme 2B). When the reaction was done, saturated salt water was added to the mixture immediately, subsequently a lot of khaki precipitates showed up. The precipitates were filtrated, and washed by using 20 mL of absolute ethanol for three times. At last, the product of RB1 was obtained. RBH (Fig. S1) and RB1 (Fig. S2) were identified by ^1H NMR and ^{13}C NMR as well as LC-MS spectroscopy.



Scheme 2 Synthetic route of RBH and RB1.

Analytical procedure

Generally, RB1 methanol solution (0.01g/L) was mixed with different concentrations of MEL, and then phosphate buffer solution (citric acid/ disodium hydrogen phosphate, pH=4.0) was added into the mixture to adjust pH. The solution was incubated for 30 min by heating in water bath at 60 $^{\circ}\text{C}$. Herein, we chose 530 nm as the excitation wavelength, and an emission band peak at 590 nm appeared and obviously increased with increasing concentrations of MEL. The free RB1 was weakly fluorescent, so the calibration curve for MEL was established up by the relationship between fluorescence intensities (F) of RB1 and the concentration (C) of MEL.

Enrichment procedure

MIPs were added into a centrifugal tube and then activated by using methanol (4.0 mL) and water (4.0 mL) in sequence. Then the supernatant was discarded after centrifugation. Then 4.0 mL of spiked milk samples of MEL was put into another centrifugal tube and 16.0 mL of ultrapure water (or acetonitrile or methanol or ethanol or methanol aqueous) was added as the extractant. When the extraction was finished, the mixture was centrifuged and protein precipitation was discarded. Afterwards, the MIPs were added, and then the mixture was stirred for 30min, the enrichment was completed, the MIPs contained MEL were separated quickly from the mixed solution by centrifugation, after that, the MIPs contained MEL were cleaned with 2.0 mL of 20% methanol aqueous for the sake of eliminating the interference. Then the MEL was eluted from MIPs with 6 \times 1 mL of methanol-acetic (95:5) under ultrasonic to improve the recoveries during each elution process. The eluate was collected and dried at 50 $^{\circ}\text{C}$ by using a nitrogen blowing instrument, the residue was then redissolved with 4 mL of methanol, and detected by using RB1with fluorescence method.

Application

All the selected pure milk samples were free of melamine from local supermarket, and the spiking concentrations for MEL were 1 and 5 mg/L respectively. Briefly, 4 mL of pure milk was extracted with 16mL of ultrapure water. After the protein was discarded through centrifuging, 120mg MIPs were added to the solution and stirred for 30min. MIPs were collected from the solution, followed by cleaned with 2.0 mL of 20% methanol aqueous and eluted with 6 \times 1 mL of methanol-acetic (95:5). The eluate was collected and dried at 50 $^{\circ}\text{C}$, the residue was then re-dissolved with 4 mL of methanol, and detected by using RB1 with fluorescence method.

Results and discussion

Characterization

Fig. 1 shows the SEM images of MIPs and NIPs. As exhibited, the MIPs seemed rough and dense compared to the NIPs. The influence of the template molecule on the surface topography is obvious. The more uniform particles of MIPs are very helpful for the adsorption of MEL than NIPs.

Fig. 2A shows the weight curves of MIPs and NIPs. In this research, MIPs and NIPs were heated from 30 $^{\circ}\text{C}$ to 700 $^{\circ}\text{C}$

under nitrogen. MIPs or NIPs had three weight loss gradations. Firstly, the initial loss (30-100 °C) was mainly due to the release of physically adsorbed water. Second gradation around 100 to 260 °C, the rate of weight loss for MIPs or NIPs was very slow, which indicated that the polymers were gradually decomposed. However, more severe rate of weight loss appeared at temperatures ranging from 260 to 450 °C. The weight loss was 30% for MIPs at 327 °C and for NIPs at 274 °C. As showed in Fig. 2B, the peak temperature could reflect the fastest rate of decomposition of polymers. The amount of remaining materials was 43.57% for MIPs at 372 °C, whereas it was 42.62% for NIPs at 326 °C. Thus, compared with NIPs, MIPs showed better thermal stability.

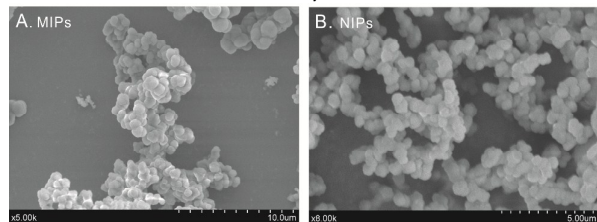


Fig. 1 SEM images of MIPs (A) and NIPs (B).

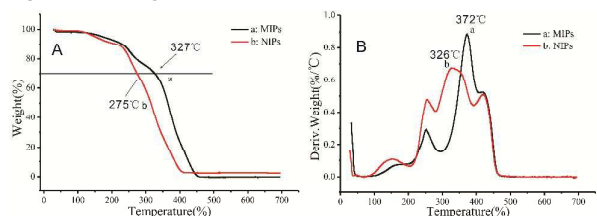


Fig. 2 Weight analysis curves of MIPs and NIPs. (A) Thermal Gravity Analysis (TG). (B) Differential thermal gravity (DTG).

Static adsorption and adsorption kinetics evaluation

Both static adsorption and adsorption kinetics experiments were applied to evaluate the combining abilities of the polymers. Fig. 3A and B show the experimental adsorption isotherms of MEL onto two types of MIPs and NIPs, respectively. One type polymer was prepared with nano-CaCO₃ as porogen, another without nano-CaCO₃. The curves plotted in Fig. 3A shows that the equilibrium adsorption amounts obviously increased with the increasing of original concentration of the MEL. When the original concentration of MEL reached to 0.6 mmol/L, the adsorption amount of NIPs became stable, but the adsorption amount of MIPs still maintained a growth trend. In addition, MIPs exhibited a significantly higher adsorption capacity than the NIPs under the same condition. The imprinting factor, which is usually applied to characterize the selectivity of MIPs, and calculated by $Q_{\text{MIPs}}/Q_{\text{NIPs}}$, is 3.072 for the present MIPs. Fig. 3B shows that the polymers had the same tendency compared to the polymers with nano-CaCO₃ as porogen, whereas the quantity of adsorption was slightly lower than that of the later ones under the same condition.

In order to measure the combining rate of MIPs or NIPs for MEL, the concentration of MEL was fixed in 0.9 mmol/L and static equilibrium binding assay was used to determine adsorption at different time intervals. Fig. 3C shows that the

polymers with nano-CaCO₃ as porogen reaching to the adsorption equilibrium within 30 min. Fig. 3D shows that the combining rate of the polymers without nano-CaCO₃ as porogen became slow and equilibrium time was three times that of the polymers with nano-CaCO₃ as porogen. This is due to nano-CaCO₃ could also be removed together with the template while eluting in the preparation of the polymer, and thus left the cave in polymers to accelerate the rate of mass transfer. Polymers mentioned later were all prepared with nano-CaCO₃ as porogen.

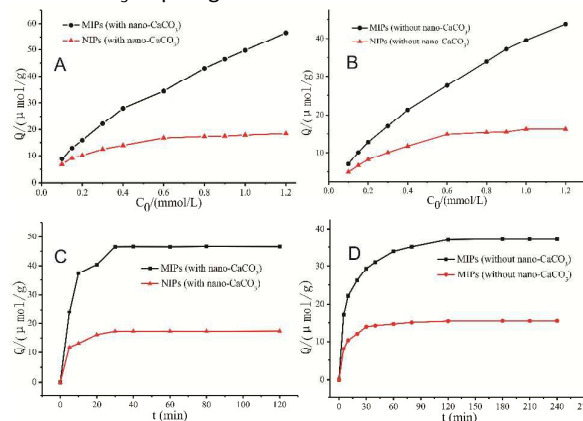


Fig. 3 (A) Isotherm of MEL adsorption on the polymers with nano-CaCO₃ as porogen. (B) Isotherm of MEL adsorption on the polymers without nano-CaCO₃ as porogen. (C) Effect of adsorption time on amounts of adsorption on the polymers with nano-CaCO₃ as porogen. (D) Effect of adsorption time on amounts of adsorption on the polymers without nano-CaCO₃ as porogen. Experimental conditions: the volume of solution: 4 mL; mass of polymers: 20 mg.

Scatchard analysis

In the study of molecular imprinting, scatchard model was commonly used to further evaluate the binding specificity. As can be seen from Fig. 4A, the relationship between Q/C and Q was obviously nonlinear according to the scatchard equation, which indicated that the MIPs binding site of MEL was heterogeneous.²² But there were two distinct parts with good linear relation in the two ends of the graph, which suggested that the MIPs had two main classes of binding sites with different adsorption properties. The two linear regression equations were fitted according to the relationship of two segments linear. The linear regression equation for the left part of the curve was $Q/C = -2.947Q + 184.3$, the K_d (equilibrium dissociation constant) and Q_{max} (maximum adsorption capacity) were calculated to be 0.3393 mmol/L and 62.53 μmol/g, respectively. The right part of the curve was $Q/C = -0.8523Q + 109.5$, the K_d and Q_{max} were calculated to be 1.173 mmol/L and 128.4 μmol/g, respectively. This phenomenon was presumably owing to the presence of multiple interactions between the template molecule and the functional monomer, which could form a variety of different compositions. Different types of complexes lead to form different properties recognition sites in the MIPs.

The combining of MEL to NIPs was also tested in the same way. As can be seen from Fig. 4B, the relationship between Q/C and Q was obviously linear, the linear regression equation was $Q/C = -7.0866Q + 145.8671$. The K_d and Q_{max} were calculated to be 0.1411 mmol/L and 20.58 $\mu\text{mol/g}$, respectively. These results indicate that adsorption capacity of MIPs to MEL is higher than that of NIPs.

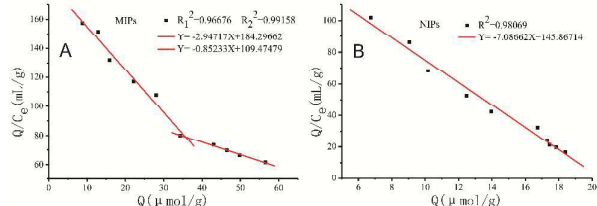


Fig. 4 Scatchard analysis of the combining of MEL onto the MIPs (A) and NIPs (B).

Selectivity and competitive measurements

MEL and structural analogues (BEN or CYR) were used to evaluate the specificity of MIPs. The selectivity experiment was carried out by adding MIPs or NIPs particles (20mg) into the centrifugal tubes containing 4 mL of 0.3 mmol/L of MEL (or BEN or CYR), respectively. As shown in Fig. 5, the amounts of MEL combined to the MIPs were significantly higher than that of the NIPs. Moreover, the MIPs displayed a better combining capability for MEL than other chemical compounds, which indicated that the MIPs showed excellent selectivity for MEL.

Competitive adsorption was evaluated by using the mixture of MEL, BEN and CYR with the concentration of each 0.3 mmol/L. As seen from Table 1, MIPs also displayed the outstanding specificity to MEL in the mixed solution. Compared to MEL, other substances including BEN and CYR lost the competitive edge, which summarized by higher α to MEL than that of other compounds in the mixture. This further proved that the synthesized MIPs had a good specificity for MEL.

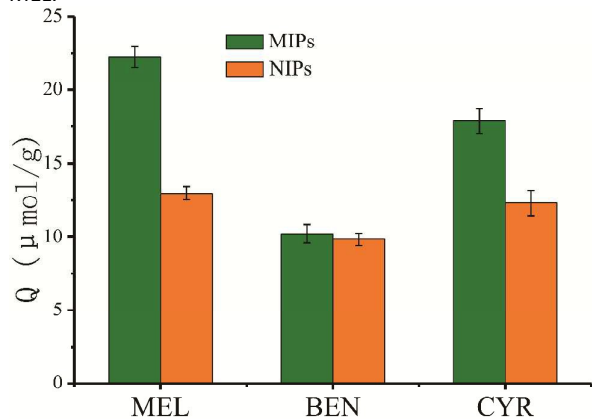


Fig. 5 The selectivity adsorption of MIPs and NIPs for each chemical compound. Experimental conditions: mass of polymers: 20 mg; volume: 4 mL; adsorption time: 24 h; adsorption temperature: 25 °C; concentration of each compound: 0.3mmol/L.

Table 1

Competitive adsorption capacities (Q) of MIPs and NIPs in the mixed solution and imprinting factor (α)

Compounds	Q_{MIPs} ($\mu\text{mol/g}$)	Q_{NIPs} ($\mu\text{mol/g}$)	α
MEL	16.02	6.831	2.345
BEN	5.023	4.603	1.091
CYR	10.13	6.726	1.506

Fluorescent detection of MEL

The changes of fluorescence spectra with the increase of the concentration of MEL added to RB1 methanol solution are shown in Fig. 8. When the maximum excitation wavelength was chosen at 530 nm, the maximum emission peak appeared at 590nm. The inset in Fig. 6 shows the fluorescence intensity of RB1 displayed an outstanding linear relationship to the concentration of MEL in the range of $6.25 \times 10^{-4} - 8 \times 10^{-2}$ mmol/L, which indicated that MEL could be accurately tested within a certain range based on the linear equation. The possible reaction principle was shown in Fig. 7. When MEL was added into the RB1 solution, a ring-opening reaction was triggered. In the acid system, hydrogen ion could promote unstable compound hydrolysis, which led to the release of strong fluorescence. The limit of detection (LOD) of the present approach was 1.55×10^{-4} mmol/L by adopting $3\delta/S$ (a signal to noise ratio of 3), where δ is the standard deviation of the blank solution, and S is the slope of the linear calibration curve. For the sake of comparison, the previously reported approaches^{8, 9, 23-25} for the determination of MEL were summarized in Table 2. It highlights that the present approach provided a much lower detection limit.

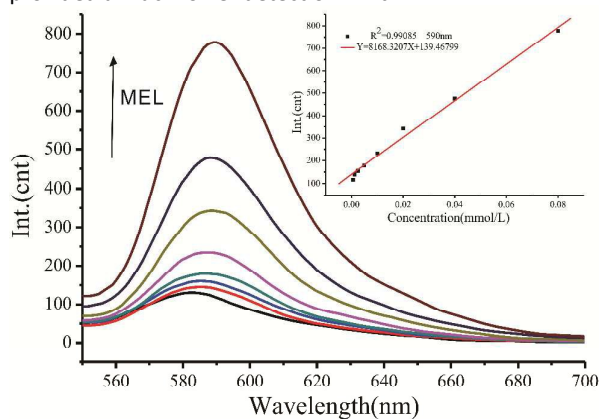


Fig. 6 Fluorescence spectra of RB1 methanol solution with the increase of the concentration of MEL ($6.25 \times 10^{-4} - 8 \times 10^{-2}$ mmol/L). Inset: the curve of the linear calibration curve.

Table 2

Comparison of different approaches for examination of MEL

Approaches	Linear range (mmol/L)	LOD (mmol/L)	References
SERS	$5.00 \times 10^{-3} - 5.00 \times 10^{-2}$	1.2×10^{-2}	9

ESI-MS	3.97×10^{-3} - 7.94×10^{-2}	7.94×10^{-4}	8
Colorimetric	3.90×10^{-4} - 3.97×10^{-3}	2.38×10^{-4}	23
Fluorescence	3.20×10^{-5} - 5.00×10^{-4}	1.80×10^{-4}	24
Visual and absorption spectroscopic	4.76×10^{-3} - 3.33×10^{-1}	3.17×10^{-3}	25
Fluorescence	6.25×10^{-4} - 8×10^{-2}	1.55×10^{-4}	This work

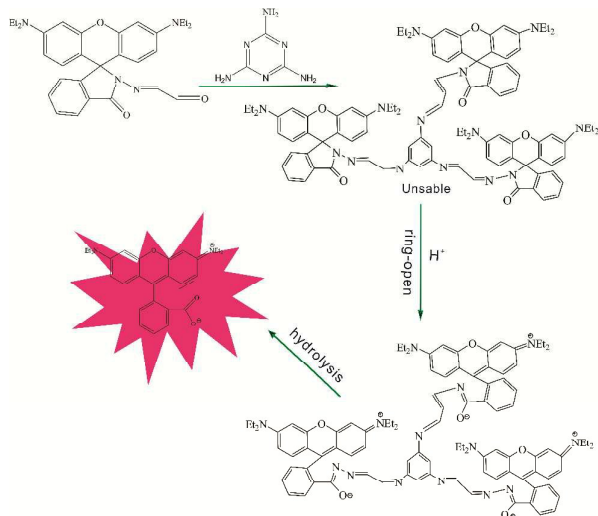


Fig. 7 The possible reaction principle of fluorescent examination for MEL

Optimization of extraction conditions

In order to evaluate the ability of MIPs for enrichment and separation of MEL from pure milk, several factors including extraction solvent, amounts of MIPs, adsorption time and elution solution were investigated. The content of MEL in elution was detected by using RB1. When one factor was changed, the other factors were fixed.

A. Extraction solvent

Extraction solvent has a significant impact on rebinding of the target molecules. Several different Extraction solvents including water, methanol aqueous (50%), methanol, acetonitrile and ethanol were taken into account. As seen from Fig. 8 (A), water was magically the optimum extraction solvent at a recovery rate of $89.05\% \pm 1.49\%$. It may be explained that MEL molecule is not easily dissolved in water than in other solvents, which is favorable for MIPs to take MEL away from water.

B. Amounts of MIPs

In order to obtain the maximum recovery rate with the minimum amounts of MIPs, different amounts of MIPs ranging from 20 to 140 mg were evaluated. As seen from Fig. 8 (B), the rate of recovery increased with the increase of amounts of MIPs ranging from 20 to 120 mg, whereas the rate of recovery decreased slightly when the amounts were 140 mg. The results demonstrated that increasing the amounts of MIPs were not

much helpful to improve the recovery, so 100 mg MIPs were just right.

C. Adsorption time

Different adsorption times ranging from 10 to 50 min were evaluated respectively. As seen from Fig. 8 (C), 30 min might be a better option due to less time and larger recovery rate. So 30 min was chosen to extract, which offered the recovery rate of $88.17\% \pm 0.99\%$.

D. Elution solution

Elution solution is also an important factor to affect the recovery rate. For the sake of obtaining the maximum recovery rate, different kinds of elution solution including methanol, ethanol, acetonitrile, water and methanol-acetic (95:5) were evaluated. As seen from Fig. 8 (D), methanol-acetic (95:5) could provide the satisfactory recovery.

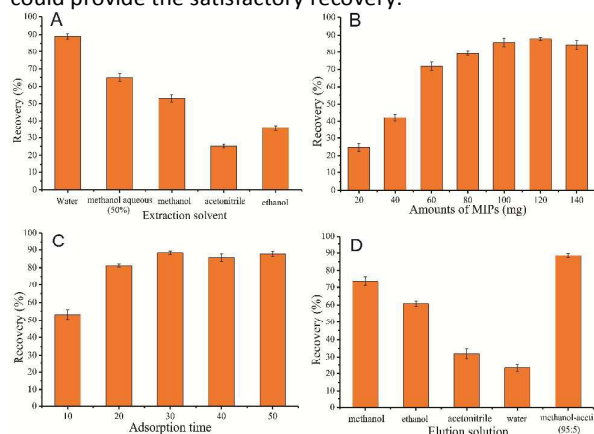


Fig. 8 Optimization of extraction conditions ($n=3$). (A) The influence of extraction solvent on the recovery of MEL. (B) The influence of amounts of MIPs on the recovery of MEL. (C) The influence of adsorption time on the recovery of MEL. (D) The influence of elution solution on the recovery of MEL.

Validation

In order to demonstrate the applicability of this proposed approach in real sample detection, the recovery test was carried out by spiking MEL into pure milk samples at two levels of 1 and 5 mg/L (about 7.936×10^{-3} and 3.968×10^{-2} mmol/L). Table 3 shows that the recovery of spiked samples varied from 86.48 to 89.12% and the RSDs varied from 3.18 to 4.91%, respectively. It could be seen that the proposed fluorescence sensing approach based on the MIPs enrichment was highly feasible.

Table 3

Detection of MEL in milk samples				
Sample	Added (mg/L)	Found (mg/L)	Recovery (%)	RSD (%) ($n=3$)
Milk	1	0.8648	86.48%	4.91%
	5	4.456	89.12%	3.18%

Conclusions

In summary, we provided a satisfactory approach relied on the use of MIPs with nano-CaCO₃ as porogen for enrichment and separation of MEL from milk samples. Notably, MEL eluted from the MIPs was detected by fluorescent chemosensor of RB1. The prepared MIPs exhibited to be selective and efficient for enrichment of MEL, and the imprinting factor of 3.072 could be obtained. The synthesized fluorescent chemosensor of RB1 showed to be sensitive for MEL detection, and displayed an outstanding linear relationship to the concentration of MEL in the range of 6.25×10^{-4} - 8×10^{-2} mmol/L. Integrating the advantages mentioned above, this system of detection of MEL was in good performance.

Acknowledgements

The authors are grateful for the financial support provided by the Ministry of Science and Technology of China (Project No.2012AA101609-2) and the National Natural Science Foundation of China (Project Nos. 21375094 and 31225021).

Notes and references

- H. Guan, J. Yu and D. Chi, *Food Control*, 2013, **32**, 35-41.
- J. Zhang, M. Wu, D. Chen and Z. Song, *Journal of Food Composition and Analysis*, 2011, **24**, 1038-1042.
- H. Yan, X. Cheng, N. Sun, T. Cai, R. Wu and K. Han, *Journal of Chromatography B*, 2012, **908**, 137-142.
- Y. L. Ji, X. W. Chen, Z. B. Zhang, J. Li and T. Y. Xie, *Journal of separation science*, 2014, **37**, 3000-3006.
- A. Fashi, M. R. Yafthian and A. Zamani, *Food Chemistry*, 2015, **188**, 92-98.
- J. Li, H. Qi and Y. Shi, *J Chromatogr A*, 2009, **1216**, 5467-5471.
- G. Venkatasami and J. R. Sowa, *Anal Chim Acta*, 2010, **665**, 227-230.
- S. K. Kailasa and H. Wu, *J Ind Eng Chem*, 2015, **21**, 138-144.
- Y. Hu, S. Feng, F. Gao, E. C. Y. Li-Chan, E. Grant and X. Lu, *Food Chem*, 2015, **176**, 123-129.
- J. Xia, N. Zhou, Y. Liu, B. Chen, Y. Wu and S. Yao, *Food Control*, 2010, **21**, 912-918.
- B. The Huy, M. Seo, X. Zhang and Y. Lee, *Biosensors and Bioelectronics*, 2014, **57**, 310-316.
- X. Cao, F. Shen, M. Zhang, J. Guo, Y. Luo, X. Li, H. Liu, C. Sun and J. Liu, *Food Control*, 2013, **34**, 221-229.
- M. Zhang, X. Cao, H. Li, F. Guan, J. Guo, F. Shen, Y. Luo, C. Sun and L. Zhang, *Food Chem*, 2012, **135**, 1894-1900.
- S. Han, S. Zhu, Z. Liu, L. Hu, S. Parveen and G. Xu, *Biosensors & bioelectronics*, 2012, **36**, 267-270.
- S. Chou and M. Syu, *Biomaterials*, 2009, **30**, 1255-1262.
- X. Pan, P. Wu, D. Yang, L. Wang, X. Shen and C. Zhu, *Food Control*, 2013, **30**, 545-548.
- D. CUNLIFFE, A. KIRBY and C. ALEXANDER, *Adv Drug Deliver Rev*, 2005.
- Z. Zhang, Z. Cheng, C. Zhang, H. Wang and J. Li, *Journal of Applied Polymer Science*, 2012, **123**, 962-967.
- M. Curcio, F. Puoci, G. Cirillo, F. Iemma, U. G. Spizzirri and N. Picci, *Journal of agricultural and food chemistry*, 2010, **58**, 11883-11887.
- A. Khelifi, S. Gam-Derouich, M. Jouini, R. Kalfat and M. M. Chehimi, *Food Control*, 2013, **31**, 379-386.
- P. Li, G. Ding, Y. Deng, D. Punyapitak, D. Li and Y. Cao, *Free Radical Bio Med*, 2013, **65**, 224-231.
- X. Song, J. Li, J. Wang and L. Chen, *Talanta*, 2009, **80**, 694-702.
- J. Xin, L. Zhang, D. Chen, K. Lin, H. Fan, Y. Wang and C. Xia, *Food Chem*, 2015, **174**, 473-479.
- Q. Wu, Q. Long, H. Li, Y. Zhang and S. Yao, *Talanta*, 2015, **136**, 47-53.
- H. Cai, X. Yu, H. Dong, J. Cai and P. Yang, *J Food Eng*, 2014, **142**, 163-169.